

Influence of the Luminance L^* during Color Segmentation in the $L^*a^*b^*$ Color Space

Rodolfo Alvarado-Cervantes¹, Edgardo M. Felipe-Riveron², Vladislav Khartchenko²,
Oleksiy Pogrebnyak²

¹ Universidad Nacional Autónoma de Mexico, Centro de Investigaciones Teóricas,
Facultad de Estudios Superiores Cuautitlan,
Mexico

² Instituto Politécnico Nacional, Centro de Investigacion en Computacion,
Mexico

rodolfo.alvarado.cervantes@gmail.com; edgardo@cic.ipn.mx; vlad@unam.mx;
olek@pollux.cic.ipn.mx

Abstract. In this paper a study of the influence of luminance L^* at the $L^* a^* b^*$ color space during color segmentation is presented. The behavior of different color image segmentation algorithms is studied, in particular, the techniques based on only the Euclidean metric of a^* and b^* and an adaptive color similarity function defined as a product of Gaussian functions in a modified HSI color space. For the evaluation purposes, synthetic images that accurately assess the performance of the color segmentation were particularly designed. The testing system can be used either to explore the behavior of a similarity function (or metric) in different color spaces or to explore different metrics (or similarity functions) in the same color space. From the obtained results it follows that the color parameters a^* and b^* are not independent on the luminance parameter L^* as one may initially assume.

Keywords: Color image segmentation; $L^*a^*b^*$ color space; color metrics; color segmentation evaluation; synthetic color image generation.

1 Introduction

Image segmentation consists of entire image partitioning into different regions, which are similar in some predefined manner. It is an important and difficult task in image analysis and processing. All subsequent steps such as object recognition depend on the quality of segmentation [1].

For some time, the development of segmentation algorithms attracted remarkable consideration but the relatively fewer efforts on their evaluation and characterization [2, 3, 4, 5]. None of the published automatic segmentation algorithms is generally applicable to all types of images and different algorithms are not equally suitable for particular applications. For these reasons, the evaluation of different segmentation

techniques and their characterization are very important subjects in the study of segmentation [3, 5].

Perceptually uniform color spaces such as $L^*a^*b^*$, with the Euclidean metric to quantify color distances are commonly used in color image segmentation of natural scenes using histogram based or clustering algorithms among others [1].

To evaluate the segmentation performance of the Euclidean metric in the $L^*a^*b^*$ color space, we designed a system that generates synthetic color images and the associated ground truth (GT) and evaluates the results with Receiver operating characteristics (ROC) curves [7]. The synthetic images were designed to evaluate the efficiency of achieved color information from given segmentation algorithms and are explained in detail in Section 3. A comparative study with an adaptive color similarity function defined as a product of Gaussian functions in a modified HSI color space [6] is presented in Section 4. Finally, conclusions are given in Section 5.

2 Previous Works

The first comprehensive survey on image segmentation evaluation methods is presented in [2]. It brings a coherent classification of existing methods at the time. An up to date of 5 years of progresses in the subject is presented in [3] after the first survey. Another actualization is presented 5 years later [5], embracing together the principal methods of segmentation evaluation available until 2007.

In [4] a way to design synthetic images and a corresponding GT for evaluating segmentation algorithms is presented. They introduce a general framework and general design considerations. Also, an evaluation system for generating synthetic gray level images taking into account their design considerations is presented.

3 Design of Synthetic Images for Benchmark Testing

In [4] the authors present three important design considerations for creating synthetic images: 1. Synthetic images should be appropriate for a quantitative study and should allow objective evaluations of their properties; 2. The synthetic images should reflect the main features of real images, i.e. corruption factors, such as noise and blurring, variation of parameters such as size, shape, etc.; 3. The system should allow the generation of images with progressive variations of each parameter. In this way the study of the influence of each individual parameter is possible.

Comparative tests between an adaptive color similarity function [6] and the Euclidean metric in the $L^*a^*b^*$ color space [8] were performed. The manner in which the tests were implemented is as follows:

In the case of the $L^*a^*b^*$ color space, the RGB image was previously transformed to $L^*a^*b^*$ color space discarding in all cases the luminance L^* in order to calculate the Euclidean distance on the planes a^*b^* (color information) independently of the illumination. Then, the centroids (average of the values a^* and b^*) representing the colors of the figure and the background in the color space $L^*a^*b^*$ were calculated. Details are shown in [8].

For the adaptive similarity function [6] the following steps were performed:

1. Samples of both background and figure were taken, from which centroid and standard color dispersion were calculated. Details can be consulted in [6].
2. The 24-bit RGB image (true color) was transformed into a modified HSI color space.
3. For each pixel, the similarity function for the centroids of object and background was calculated creating two color similarity images (CSI) [6].
4. Each pixel of the RGB image was classified by calculating the maximum value for each pixel position between the CSI images of the object and that of the background.

The base shape of the synthetic test image was created with the following features:

1. Concave and convex sections were included in order to make it more representative of real images, such as natural flowers.
2. Extreme omnidirectional curvature in the entire image was selected to hinder edge detection by mask edge detectors.
3. The object was centered in the image.

The resulting flower-shaped object in the image is considered as the object of interest and as the ground truth GT in all subsequent tests (Figure 1 left).

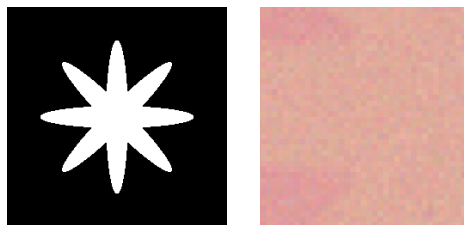


Fig. 1. Flower-shaped ground truth (left) and an image zoomed showing the Gaussian noise introduced (right).

In addition to this object of interest, several features were imposed in order to hinder its color-based segmentation:

1. Low contrast. The contrast between the object and the background in all images was very low for an observer, including some in which at a first glance the user cannot see the difference (e.g. Flower 5 in Figure 2). The difference between the color characteristics of the object of interest and the background we call “Delta” and it occurs at different directions of the HSI space. The tests were performed in color quadrants 0, 60, 120, 180, 240 and 300 degrees.

2. Blurred edges by an average filter. A sliding mean filter of size 3 x 3 pixels is applied to the whole image in order to blur the corners and to make detection of the object more difficult; this averaging is done before the introduction of Gaussian noise.

3. Introduction of Gaussian noise with SNR value = 1. The noise was applied to each RGB channel separately, and later we assembled the channels to create the noisy RGB color image with noise. Figure 1 right shows an example of such a noisy image.

The basic colors selected for both object and background were based on maintaining constant intensity at 0.5 and saturation at 0.3 and only varying the hue. Hue was selected as the parameter because its change integrates three RGB color channels together, making it more difficult to be processed by extending grayscale

techniques on each color channel, thus forcing the segmentation algorithms in evaluation to use the color information holistically.

Samples of pixels corresponding to the figure were obtained by two squares of 2 x 2 pixels starting at the pixel (84, 84) and (150, 150). Samples for background pixels were obtained by two squares of 2 x 2 pixels starting at pixel (15, 15) and (150, 180).

The images were generated in the sectors 0, 60, 120, 180, 240 and 300 degrees corresponding to the images flower_0, flower_1 ... flower_5 (Figure 2). To each of these test images we later applied a faded shadow in increments of 10% at each step.

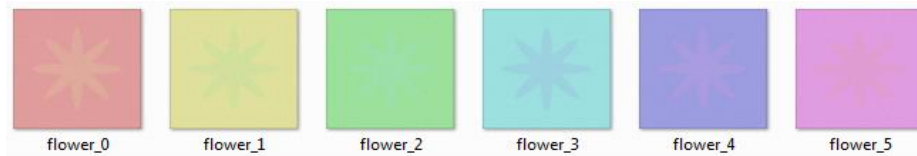


Fig. 2. Testing with Low Saturation with Delta in HUE.

A shadow fading was applied to all noisy blurred images with the light center in the fixed coordinates (150,150) in images of 256 x 256 pixels. It was applied gradually with 10% increments at each step. Figure 3 shows this for Flower 0.

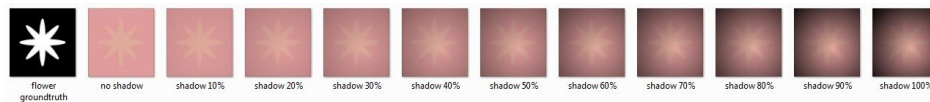
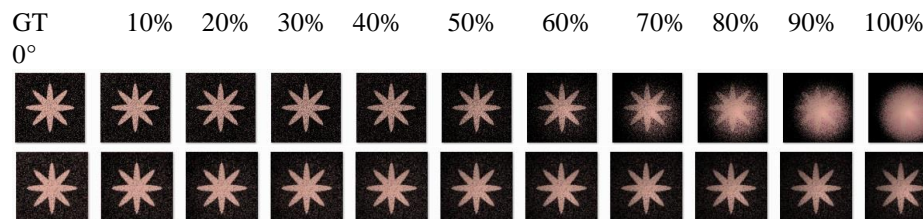


Fig. 3. Example in color quadrants with a faded shadow applied at 0 degrees.

4 Results and Discussion

In this section we show the results in terms of TP (true positives) and FP (false positives) plotted against the level of shadow fading, representing by 10% of increment at each step. The first position means no shadow and position 11 means 100% shadow fading. All the images had the same post-processing: elimination of areas smaller than 30 pixels and a morphological closing with a circular structuring element of radius equal to two pixels.

The results of the application with the solution given by [6] of the color image segmentation with a different level of shadow fading (shown in every even row) compared with those obtained with the Euclidean metric in the $L^*a^*b^*$ rejecting L^* (shown in every odd row) are included in Figure 4 for each color quadrant (0° , 60° , 120° , 180° , 240° and 300°) and at 10% increments of the shadow fading.



Influence of the Luminance L^ during Color Segmentation in the $L^*a^*b^*$ Color Space*



Fig. 4. Results of the color segmentation achieved between the Euclidean metric of a^* and b^* (top rows of each color) and the adaptive color similarity function (bottom rows of each color), for each color quadrant (0° , 60° , 120° , 180° , 240° and 300°) and at 10% increments of shadow fading in each step.

As it is shown in the graphs of Figure 5 and in coincidence with the visual analysis of the corresponding flower (Figure 4), segmentation failures in the $L^*a^*b^*$ space (right) start at different levels of faded shadow, whereas the adaptive color similarity function [6] is practically immune to the faded shadow (left).

We can see three general trends in the FP behavior in Figure 5 right (See Table 2): 1. Increase in an angle of approximately 45° in cases of Flower 0 and Flower 3 (with diamond marker); 2. Slowly and progressively increases in cases of Flower 1 and Flower 4 (with square marker) and 3. Sharply increases in cases of Flower 2 and

Flower 5 (with circular marker). The behavior is repeated every 180 degrees and coincides with the opponent color positions (yellow-blue for example).

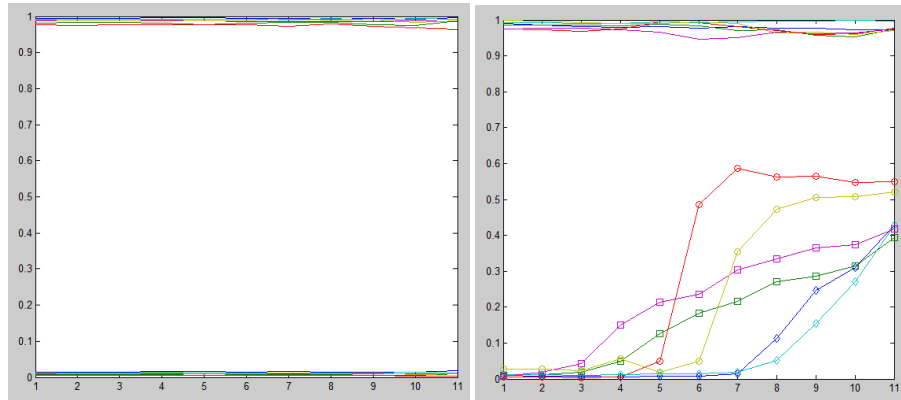


Fig. 5. Plots of the color similarity function [6] (left) and the Euclidean metric in $L^*a^*b^*$ rejecting L^* (right).

Figure 6 shows details of the curves related to TP and FP of the color similarity function [6], with the following color code: Flower 0 (blue), Flower 1 (green), Flower 2 (red), Flower 3 (cyan), Flower 4 (purple) and Flower 5 (yellow). Variations in curves are lower than 1%.

To obtain a representative ROC curve illustrating behavior of the Euclidean metric in the $L^*a^*b^*$ space (rejecting L^*) compared to the color similarity function [6] in all color sectors under study, we calculated the average TP and FP for all color flowers, obtaining the results shown in Figure 7.

Table 2. Observations concerning the behavior of the plot curves of the two colour metrics.

Flower	Line Color	Euclidean metric in $L^*a^*b^*$ rejecting L^*	Color similarity function [6]
0	Blue	60% (position 7) Increases at 45°	Immune
1	Green	30% (position 4) Increases slowly and progressively	Immune
2	Red	40% (position 5) Sharply increases	Immune
3	Cyan	70% (position 8) Increases at 45°	Immune
4	Purple	20% (position 3) Increases slowly and progressively	Immune
5	Yellow	50% (position 6) Sharply increases	Immune

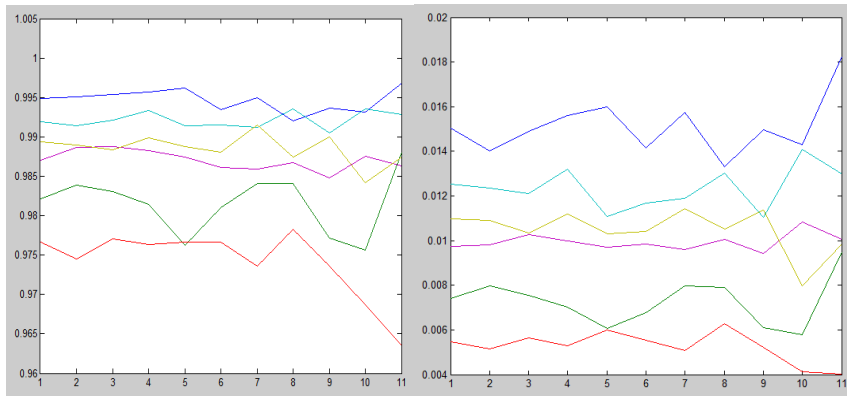


Fig. 6. Details of TP (left) and FP (right) of the color similarity function [6].

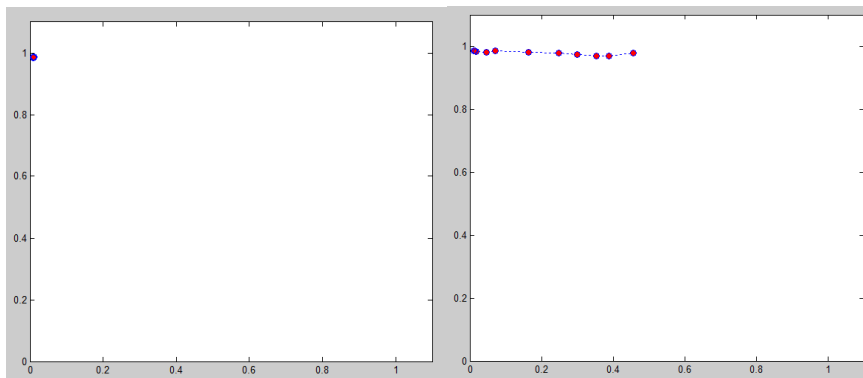


Fig. 7. ROC curve of the color similarity function [6] (left) and the Euclidean metric in the $L^*a^*b^*$ rejecting L^*

In the ROC curve corresponding to the average of TP and FP of all flowers, it can be seen that the results of the adaptive similarity function are maintained in the high efficiency area (coordinate 0, 1) while the color segmentation in $L^*a^*b^*$ space progressively moves away from the high efficiency area.

The $L^*a^*b^*$ results keep stable initially and later slowly and progressively moves to the upper right area of the ROC curve that can be thought of as the “liberal” side (coordinate 1, 1) as they make positive classifications, and, although there is weak evidence that almost all positives were classified properly, they have a high rate of false positives.

5 Conclusions

Regarding the evaluation of the color segmentation method with really difficult conditions, we can notice that the adaptive color similarity function performed well in all tests and remained close to the high efficiency zone of the ROC curves

(coordinates 0,1) without noticeable changes when the level of faded shadow increases as shown in the corresponding PLOT curves.

The segmentation algorithm using the $L^*a^*b^*$ color space and discarding L^* in calculating the Euclidean distance, suffered errors in all cases. It manifested in different degrees and at different levels of faded shadow (20% to 80%). Three types of trends or recurring symmetries can be noticed in sectors with 180 degrees of difference: 1. Rise of the curve gradually (Flowers 1 and 4); 2. Rise abruptly (Flowers 2 and 5), and 3. Increase near at 45° angle (Flowers 0 and 3).

As it can be seen from the results of both direct segmentation, and from PLOT & ROC curves, that the adaptive color similarity function in all cases exceeded the Euclidean distance in color space $L^*a^*b^*$ and discarding L^* . The similarity function segmentation method performed well in all cases with rates higher than 95% of true positives (TP) and false positive (FP) rate less than 3% on average.

According to the experiment results we believe that keeping high values of TP increased only from the FP is due to the position of the center of the shadow fading in (150, 150). If this position is moved away from the object of interest, we can reduce the quantity of TP.

For future work we wish to evaluate different color zones like of different saturations, gray images, and with delta saturation among others. Our testing system can be used either to explore the behavior of a similarity function (or metric) in different color spaces or to explore different metrics (or similarity functions) in the same color space. Instead of exchanging color spaces in the experiments, it would only be necessary to exchange the metric or the similarity function.

It can be noticed that the non-consideration of the luminance parameter L^* in calculating Euclidean distance (in each pixel of the object or of the background) did not made it immune to changes in lighting; so simple shadow can alter the quality of the results, concluding from them that the parameters a^*b^* from the color space $L^*a^*b^*$ are not independent of the L^* parameter as one might suppose.

Acknowledgements. The authors of this paper wish to thank the Centro de Investigaciones Teóricas, Facultad de Estudios Superiores Cuautitlan (FES-C); Universidad Nacional Autónoma de México (UNAM), México; PAPIIT IN112913 and PIAPIVC06, UNAM; Centro de Investigación en Computación (CIC); Secretaría de Investigación y Posgrado (SIP); Instituto Politécnico Nacional (IPN), México, and CONACyT, México, for their economic support to this work.

References

1. Plataniotis, K.N., Venetsanopoulos, A.N.: Color Image Processing and Applications. First Edition, Springer, Berlin Heidelberg Germany, 354 p. (2000)
2. Zhang, Y.J.: A Survey on Evaluation Methods for Image Segmentation. Pattern Recognition, Vol. 29, No 8, pp. 1335–1346 (1996)

3. Zhang, Y.J.: A review of recent evaluation methods for image segmentation. Proceedings of the 6th International Symposium on Signal Processing and Its Applications, pp. 148–151 (2001)
4. Zhang, Y.J., Gerbrands, J.J.: On the Design of Test Images for Segmentation Evaluation. Proceedings EUSIPCO, 1, pp. 551–554 (1992)
5. Zhang, Y.J.: A Summary of Recent Progresses for Segmentation Evaluation. In: Zhang Y.J., Advances in Image and Video Segmentation. IGI Global Research Collection, Idea Group Inc (IGI), pp. 423–439 (2006)
6. Alvarado-Cervantes, R., Felipe-Riveron, E.M., Sanchez-Fernandez, L.P.: Color Image Segmentation by means of a Similarity Function. In: 15th Iberoamerican Conference on Pattern Recognition, CIARP 2010, Rodolfo Alvarado-Cervantes, Edgardo M. Felipe-Riveron y Luis P. Sánchez-Fernandez, I. Bloch and R.M. Cesar, Jr. (Eds.): Sao Paulo, Brazil, LNCS 6419, pp. 319–328, Springer, Heidelberg (2010)
7. Fawcett, T.: An introduction to ROC analysis. Pattern recognition Letters, pp. 861–874 (2006)
8. <http://www.mathworks.com/help/images/examples/color-based-segmentation-using-the-l-a-b-color-space.html> (Revised on April 27, 2015)